Mathematical Biology

Jonathan Rubin · David Terman

Analysis of clustered firing patterns in synaptically coupled networks of oscillators

Abstract. Oscillators in networks may display a variety of activity patterns. This paper presents a geometric singular perturbation analysis of clustering, or alternate firing of synchronized subgroups, among synaptically coupled oscillators. We consider oscillators in two types of networks: mutually coupled, with all-to-all inhibitory connections, and globally inhibitory, with one excitatory and one inhibitory population of oscillators, each of arbitrary size. Our analysis yields existence and stability conditions for clustered states, along with formulas for the periods of such firing patterns. By using two different approaches, we derive complementary conditions, the first set stated in terms of time lengths determined by intrinsic and synaptic properties of the oscillators and their coupling and the second set stated in terms of model parameters and phase space structures directly linked to parameters. These results suggest how biological components may interact to produce the spindle sleep rhythm in thalamocortical networks.

1. Introduction

Oscillatory behavior can take a variety of forms [10]. In one type of oscillation, exemplified by relaxation oscillations, some property of an object varies repeatedly between two distinct states. In such activity, the amount of time spent in each state greatly exceeds the time spent in the transitions between states. For example, the generation of action potentials by certain types of neurons fits into this category of behaviors. Using neuroscience terminology, we can classify the two prolonged states of such oscillators as an *active phase* and a *silent phase*, and we can refer to the rapid transition from the silent phase to the active phase as *firing*.

When objects capable of assuming two such distinct states are coupled, the state of one object influences the other objects in the resulting network. One effect seen within networks of neurons, for example, is that cells that are normally in the silent phase can be pulled into the active phase, or induced to fire, by the firing of other cells to which they are coupled (for example, see [11]). Thus, coupling between such oscillators can lead to many interesting patterns of activity.

One such activity seen in a network of coupled oscillators of the type discussed above is the formation of clusters, such that the behaviors of oscillators in a single

J. Rubin, D. Terman: Department of Mathematics, The Ohio State University, 231 W. 18th Avenue, Columbus, OH 43210, USA. e-mail: rubin@math.pitt.edu

cluster are synchronized while oscillators from distinct clusters are never simultaneously active. One reason that such patterns are of interest is that they arise in certain neurons in the thalamus, called thalamocortical relay cells, in drowsiness and shallow non-REM sleep [6], [16], [17]. In this paper, for two general classes of networks of relaxation oscillators motivated by thalamocortical neurons, we prove that certain conditions imply the existence and stability of clustered solutions. This entails consideration of two issues, namely what prevents oscillators in separate clusters from firing together and what maintains the synchrony of oscillators belonging to the same cluster. Note that the latter issue may become especially subtle when a clustered solution of a network is stable but the completely synchronous state is unstable.

The remainder of the paper is organized as follows. In Section 2, we present the models, for individual oscillators and for the dynamic coupling between oscillators, to be considered, along with some relevant notation. The models of coupling that we include are motivated by the properties of chemical synapses between neurons [7]; hence, we refer to the connections between oscillators as synaptic coupling. We introduce two different network architectures, namely a mutually coupled network and a globally inhibitory network. A mutually coupled network consists of one population of oscillators, coupled in an all-to-all manner with inhibitory synaptic coupling. Such a network has been considered in many past works; see [11] for a review of some recent results in the context of neuronal networks. A globally inhibitory network consists of two distinct populations of oscillators; one population excites the other, which in turn inhibits the first [11], [13]. It was shown in [13] that quite different pattern formation mechanisms arise in these two different architectures.

Section 2 also includes a brief introduction to some singular perturbation terminology that is useful for our analysis, including the notion of a singular solution. The idea of this geometrical dynamical systems approach is to construct singular solutions by dissecting a system of differential equations into subsystems evolving on disparate time scales. Actual solutions exist near these singular solutions under certain general hypotheses (see [9]). In the models we consider, the relevant temporal disparity exists between the slow time scale that characterizes the time oscillators spend in the active and silent phases and the fast time scale that characterizes their transitions between these phases. Geometric singular perturbation methods have been used previously to study the population rhythms of neuronal networks (for example, see [11], [13], [14], [15], [19], [20], [21]). To our knowledge, however, these techniques have generally not been applied to analyze the formation of clustered activity patterns in mutually coupled networks of oscillators with inhibitory synaptic coupling or in networks with multiple oscillator populations, such as globally inhibitory networks.

Our main focus in this work is on these globally inhibitory networks, since they model the thalamocortical architecture. In Section 3.1, we describe an example of a singular solution consisting of two clusters for such networks. Section 3.2 contains additional notation useful for analyzing clustered solutions, and Sections 3.3-3.5 present the statement and proof of an existence and stability result for a certain class of clustered solutions, along with a formula for the period of an n-cluster solution.

Section 3.6 gives results on 2-cluster solutions of a more general type, under less restrictive assumptions than the earlier sections.

Finally, in Section 4, we present a different approach to proving existence and stability, and to computing period, for antisynchronous 2-cluster solutions, which are characterized by alternation in firing of the two clusters. This approach is more directly computational, leading to qualitatively different types of existence and stability conditions than those given by the approach of the earlier sections. We demonstrate this approach first for mutually coupled networks, where the resulting conditions are the cleanest, and then discuss globally inhibitory networks. Since the existence and stability conditions in Section 3 are sufficient but not necessary, the analysis of Section 4 complements that of the earlier sections. Moreover, it yields more direct statements about the quantitative effects of certain parameters on the stability and period of clustered states. We conclude with a discussion in Section 5.

2. Models

This section contains the models that we consider in subsequent sections. We start by presenting the equations for individual oscillators. Then, we introduce the dynamics of the coupling between oscillators and the two arrangements of connections that we will consider. We will distinguish between several types of coupling; the properties of the coupling included can play an important role in pattern formation within a network. Much of this discussion follows that in Section 2 of [13].

2.1. Single oscillators

We model the individual elements of our networks as relaxation oscillators, each governed by the system

$$\begin{aligned} v' &= f(v, w) \\ w' &= \epsilon g(v, w) \end{aligned} \tag{2.1}$$

where $' = \frac{d}{dt}$, $v \in \mathbf{R}$, and $w \in \mathbf{R}^n$; for simplicity, we take $n = 1$ in our analysis (see [13] for an example with larger n). Here, ϵ is assumed to be a small parameter; hence, w represents a slowly evolving quantity. We assume that the v-nullcline, $f(v, w) = 0$, defines a cubic-shaped curve, with left, middle, and right branches, in the (v, w) phase plane. We also assume $f > 0$ ($f < 0$) above (below) this curve. Further, the w-nullcline, $g(v, w) = 0$, is a monotone decreasing curve that intersects $f = 0$ at a unique point p_0, with $g > 0$ ($g < 0$) below (above) this curve. See Figure 1.

Definition 1. *An oscillator is* **excitable** *if p_0 lies on the left branch of $f = 0$. An oscillator is* **oscillatory** *if p_0 lies on the middle branch of $f = 0$.*

Remark 1. For an excitable oscillator, p_0 is a stable rest point. The term excitable applies because the oscillator can be induced to jump to the vicinity of the right branch of $f = 0$, or fire, if sufficiently excited by some input. In the oscillatory case, (2.1) gives rise to a periodic solution for all ϵ sufficiently small, as shown in Figure 1.
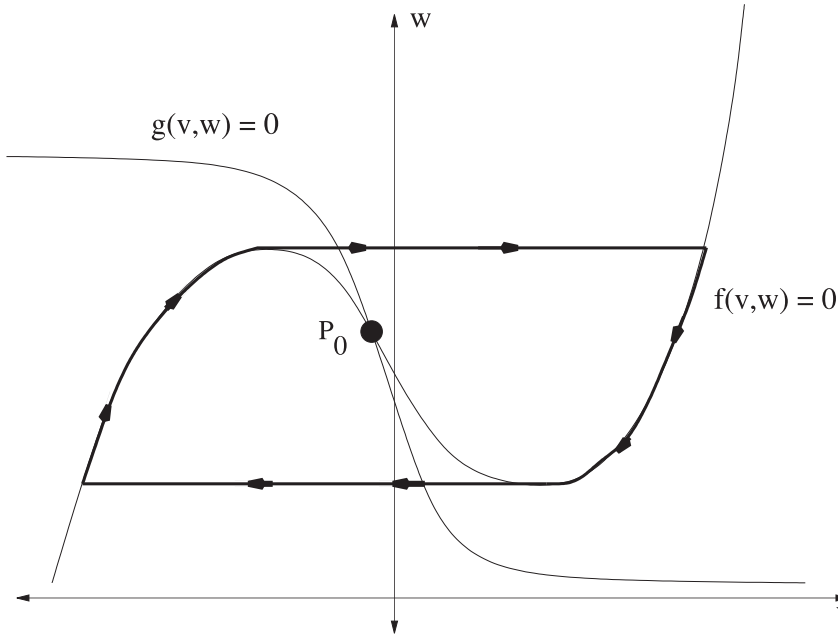
Fig. 1. Nullclines for (2.1) in the oscillatory case. The dark line shows a singular periodic solution for this system.

In singular perturbation terminology, system (2.1) represents evolution with respect to the fast time t. Setting $\epsilon = 0$ in (2.1) yields the *fast subsystem*

$$v' = f(v, w)$$
$$w' = 0$$

for which w is a parameter. Rescaling time by setting $\tau = \epsilon t$ provides the slow evolution corresponding to (2.1), namely

$$\epsilon \dot{v} = f(v, w)$$
$$\dot{w} = g(v, w) \tag{2.2}$$

where $\dot{} = \frac{d}{d\tau}$. Setting $\epsilon = 0$ in (2.2) yields the *slow subsystem*

$$0 = f(v, w)$$
$$\dot{w} = g(v(w), w)$$

which is valid as long as $f(v, w)$ can be solved for $v = v(w)$.

For neuronal models, the v-nullcline $f = 0$ describes a three-branched surface, with adjacent branches joined by *knees* (or curves of knees for $n > 1$) and $v = v_i(w)$ on the ith branch. Then, the fast subsystem governs jumps between branches of this surface, while the slow subsystem governs the flow on each branch, with v slaved to w. A fast jump occurs when a trajectory of the slow subsystem reaches a curve

of knees. The generation of an action potential by a neuron, for example, corresponds to a fast jump from the low-v branch (the silent phase) to the high-v branch (the active phase). We can thus construct a *singular solution* in the $\epsilon = 0$ limit, consisting of solutions to the slow subsystem joined by jumps between branches given by solutions to the fast subsystem; the analysis in this work deals with such singular solutions, and we refer the reader to [9] for extensions to small positive ϵ.

2.2. Coupling and architectures

We consider networks with dynamic connections between oscillators. The dynamics of the connections are motivated by models for synaptic coupling between neurons [2], [5], [22]. Such connections affect the v-evolution of the cells receiving inputs. We consider two different architectures, or arrangements of connections between oscillators in a network.

   One relatively simple architecture consists of a collection of N *mutually coupled* oscillators. In this arrangement, each oscillator is connected to all of the other oscillators in the network and to itself. The governing equations for this network are

$$v'_i = f(v_i, w_i) - g_{syn}\left(\tfrac{1}{N}\sum_{j=1}^{N} s_j\right)(v_i - v_{syn}) \quad i = 1, \ldots, N \qquad (2.3)$$
$$w'_i = \epsilon g(v_i, w_i)$$

for parameters $g_{syn} > 0$ and v_{syn} and dynamic synaptic coupling variables s_j.

Definition 2. *The coupling to the ith oscillator is* **inhibitory** *if $v_i - v_{syn} > 0$ always holds over the range of v_i values under consideration. This coupling is* **excitatory** *if $v_i - v_{syn} < 0$ always holds.*

That is, inhibitory coupling decreases v'_i, making it harder for an oscillator to fire, while excitatory coupling increases v'_i, making firing easier.

   We consider two different models for the evolution of the s_j. If an s_j is *direct*, it satisfies a first order equation of the form

$$s'_j = \alpha(1 - s_j)H(v_j - \theta_{syn}) - \epsilon K s_j. \qquad (2.4)$$

Here, H is the Heaviside step function and θ_{syn} is a threshold. The positive constants α and K are $O(1)$ with respect to ϵ and govern the rate of evolution of s_j. Note that the turn on of s_j occurs on the fast time scale while the turn off occurs on the slow time scale. This choice of rates is suggested by experimental observations in thalamocortical networks [3], [5], [18].

   A second category of dynamics characterizes *indirect* synaptic coupling, which features a delay between the crossing of the threshold θ_{syn} and the onset of its inhibitory or excitatory effect. This delay arises when secondary processes, such as G-protein activation in neuronal synapses, are needed to transmit information about the state of one oscillator to another oscillator to which it is coupled. Indirect coupling is modeled by introducing an intermediate variable x_j for each s_j [5],[13],[19]. The equations for (x_j, s_j) are

$$x'_j = \epsilon\alpha_x(1 - x_j)H(v_j - \theta_{syn}) - \epsilon K_x x_j$$
$$s'_j = \alpha(1 - s_j)H(x_j - \theta_x) - \epsilon K s_j \qquad (2.5)$$

for constants $\alpha, \alpha_x, K, K_x, \theta_x > 0$.

The other network architecture that we consider, on which much of this work focuses, involves two distinct populations of oscillators. In this *globally inhibitory* architecture, J oscillators inhibit E oscillators, which in turn excite the J. In the rhythms of interest, the oscillators within the J population are completely synchronized with each other, in which case we can model the entire J population as a single oscillator, which sends a "global inhibition" to the E population. Under this assumption, in the case of direct coupling, the system of equations corresponding to each E_i, $i = 1, \ldots, N$ is

$$
\begin{aligned}
v_i' &= f(v_i, w_i) - g_{inh} s_J (v_i - v_{inh}) \\
w_i' &= \epsilon g(v_i, w_i) \\
s_i' &= \alpha(1 - s_i) H(v_i - \theta_{exc}) - \beta s_i
\end{aligned}
\tag{2.6}
$$

with $g_{inh}, \alpha, \beta > 0$, while the system for J is

$$
\begin{aligned}
v_J' &= f_J(v_J, w_J) - g_{exc} \left(\frac{1}{N} \sum_{i=1}^N s_i \right) (v_J - v_{exc}) \\
w_J' &= \epsilon g_J(v_J, w_J) \\
s_J' &= \alpha_J(1 - s_J) H(v_J - \theta_{inh}) - \epsilon K_J s_J
\end{aligned}
\tag{2.7}
$$

with $g_{exc}, \alpha_J, K_J > 0$. We assume that $\beta = O(1)$ in (2.6); however, there is no problem extending the analysis if $\beta = O(\epsilon)$. If $v_i > \theta_{exc}$, then $s_i \to s_A \equiv \frac{\alpha}{\alpha+\beta}$ on the fast time scale. Define

$$
s_{tot} = \frac{1}{N} \sum_{i=1}^N s_i
\tag{2.8}
$$

and note that $s_{tot} \le s_A$ since each $s_i \le s_A$.

We may also take the inhibitory coupling from the J oscillators to the E oscillators as indirect. In that case, the model includes an indirect variable x_J such that the variables (x_J, s_J) evolve according to as system analogous to (2.5), namely

$$
\begin{aligned}
x_J' &= \epsilon \alpha_x (1 - x_J) H(v_J - \theta_{inh}) - \epsilon K_x x_J \\
s_J' &= \alpha_J(1 - s_J) H(x_J - \theta_x) - \epsilon K_J s_J.
\end{aligned}
$$

Remark 2. We will see that, without loss of generality, inhibition can be taken as direct for the consideration of the existence of clustered solutions. The distinction of direct versus indirect coupling is quite important, however, in the consideration of the stability of clustered solutions. In particular, indirect synapses are needed for stable synchronization of oscillators within a single cluster (see Section 3.5).

Remark 3. We analyze solutions of the model by constructing singular solutions. If g_{inh} is not too large then $\{(v, w) : f(v, w) - g_{inh} s_J (v - v_{inh}) = 0\}$ defines a cubic shaped curve for each $s_J \in [0, 1]$. We denote these curves as $\mathscr{C}_{s_J}$; curves $\mathscr{C}_0$ and $\mathscr{C}_1$ are displayed in Figure 2. Each E_i will lie on the left or right branch of one of these curves during the silent or active phase. Jumps between these phases take place when an E_i reaches a left or right knee of its respective cubic. In a similar manner, J lies on the cubic curve determined by its total synaptic input s_{tot}.
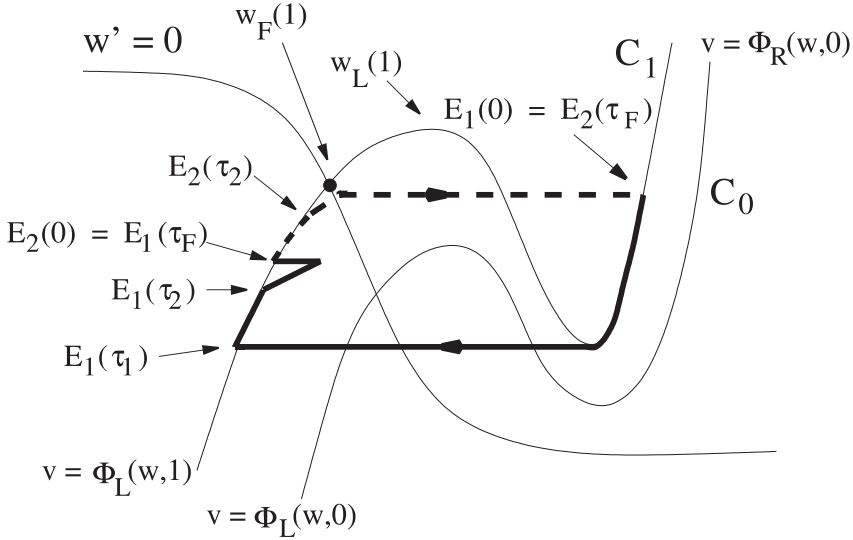
Fig. 2. Singular trajectories for both E clusters in one half-cycle of a 2-cluster solution. The solid line represents the trajectory for cluster E_1 and the dashed line that for E_2. The trajectories are superimposed on the corresponding E nullclines, with $\mathscr{C}_0$ corresponding to $s_J = 0$ and $\mathscr{C}_1$ to $s_J = 1$ as in the text.

Remark 4. The globally inhibitory model is motivated by thalamocortical networks. These networks consist of two coupled populations of cells, namely thalamocortical relay cells, which play the role of E oscillators, and thalamic reticular cells, which are the corresponding J oscillators. In these networks, spindle states, in which the J population is synchronized while the E population forms clusters, exist during drowsiness and shallow non-REM sleep.

3. Globally inhibitory networks with fast decay of inhibition

3.1. Singular orbits

In this subsection, we describe the singular trajectory corresponding to a 2-cluster solution. The number of E oscillators in the network may be arbitrary, but we assume for ease of notation that the two clusters have equal numbers of oscillators. The J oscillators are assumed to be synchronized; we may therefore consider the J population as a single J oscillator and refer to its members as a single entity J. We assume throughout that each cell, whether an E or J, is excitable for fixed levels of synaptic coupling.

As we shall see, the construction of a 2-cluster solution easily generalizes to an arbitrary number of clusters. The geometric construction will require certain assumptions, however, and a precise theorem is stated and proved in the following subsections. By considering a 2-cluster solution here, we can more easily motivate the assumptions and the statement of the main theorem that follows.

$w_J' = 0$

$S_{tot} = 0$

$S_{tot} = S_A / 2$

$J(\tau_F)$

$J(0)$

$J(\tau_1)$

$J(\tau_2)$

$J(\tau_2)$
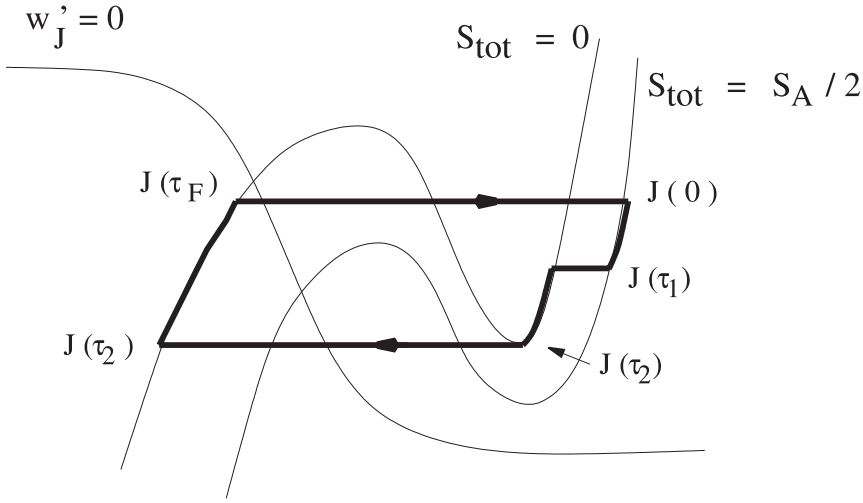
Fig. 3. Singular J trajectory for a 2-cluster solution, superimposed on corresponding nullclines.

The singular trajectories corresponding to a 2-cluster solution are illustrated in Figures 2 (E) and 3 (J). We assume that one cluster, call it E_1, jumps up to the active phase at $\tau = 0$, where τ is the slow time variable, and the resulting excitation causes J to also jump up. Since the jump up is instantaneous on the slow time scale, we can think of $E_1(0)$ as lying on the left or the right branch of the $s_J = 1$ cubic, but in any case, E_1 evolves on the right branch of the $s_J = 1$ cubic for $\tau > 0$. Similarly, J evolves on the right branch of the $s_{tot} = \frac{1}{2}s_A$ cubic for $\tau > 0$. We also assume that the other cluster, call it E_2, is silent at $\tau = 0$ and hence lies on the left branch of the $s_J = 1$ cubic.

For $\tau > 0$, each oscillator evolves along its respective branch until one oscillator reaches a knee. We will assume that the E oscillators in E_1 have shorter active phases than J, so E_1 jumps down before J does, say at $\tau = \tau_1$. The assumption that J has a longer active phase than E_1 implies that it lies above the right knee of the $s_{tot} = 0$ cubic at this time, so it continues along the right branch of the $s_{tot} = 0$ cubic until it reaches the right knee and then jumps down, say at $\tau = \tau_2$. During the time that J remains active, both E_1 and E_2 move along the left branch of the $s_J = 1$ cubic $\mathscr{C}_1$.

After J jumps down, $s_J(\tau)$ decreases on the slow time scale. If E_2 is able to reach the left knee of $\mathscr{C}_{s_J}$ for some s_J, then it fires and this completes the first half cycle of the singular solution. Suppose that this is the case and that $\tau = \tau_F$ when this occurs. Let w_i denote the w-value of all oscillators in cluster E_i. If $w_2(\tau_F) = w_1(0)$, $w_1(\tau_F) = w_2(0)$, and $w_J(\tau_F) = w_J(0)$, then the trajectories described represent one-half of a 2-cluster solution.

The analysis in Section 3.4 shows that a 2-cluster solution as described above will exist, under certain assumptions on the nonlinear functions and parameters. For example, we will need to assume that the active phase of J is not too long or too

short, compared with the active phase of the E_i. If J's active phase is too long, then the network exhibits synchronous behavior [13]. If J's active phase is too short, then the system approaches the stable quiescent state.

The singular trajectory for an n-cluster oscillation represents a natural generalization of that for the 2-cluster oscillation. In the singular n-cluster solution, if we start when J falls down, then inhibition to the E_i decays until one E cluster fires and causes J to fire; while these are active, the other $(n-1)$ E clusters evolve in the silent phase. The active E cluster falls down before J, and the E clusters then evolve in the silent phase such that each E oscillator reaches the initial position of the oscillator ahead of it in the firing sequence at the moment that J falls down again. Precise conditions for the existence and stability of such a solution are given in the next subsection.

Remark 5. The preceding construction of the singular solutions helps to motivate the assumptions and statement of the theorems in this section. For example, the 2-cluster solution can exist only if an E oscillator is able to reach the jump-up curve once it is released from inhibition after the J oscillator jumps down. We will see that this is possible only if the rate of decay of inhibition is sufficiently fast and the E oscillator recovers sufficiently in its silent phase before J jumps down.

The time an E oscillator has for recovery is related to the duration of the J oscillator's active phase. Hence, we will need to assume that K_J is sufficiently large and J's active phase is sufficiently long. We will also need to assume that the J oscillator recovers quickly in its silent phase. This is needed because once an E oscillator reaches the jump-up curve, the J oscillator must be ready to jump up in response to the firing E oscillator.

Finally, the singular construction helps to determine the number of clusters which emerge in a given network. In the construction of an n clustered solution, we have at most one cluster of E oscillators active at any particular time, with the remaining $n-1$ clusters silent. This implies that each cluster is silent for at least $n-1$ times as long as it is active. The number of clusters that can be supported depends on several factors including the duration of the J oscillator's active phase and the time it takes for inhibition to wear off before an E oscillator can reach the jump-up curve and fire. The theorems in this section give precise conditions for when an n cluster solution exists in terms of these various lengths of time.

3.2. Notation for slow phase space analysis

The following notation will be useful for the statement and proof of the theorems. Some of it is illustrated in Figure 2. Much of it is based on the approach of considering separate phase spaces for the E and J oscillators, with the dynamics in each phase space influencing that of the other as indicated in (2.6)-(2.7) [13]. Let $\mathscr{C}_{s_J}$ be the cubic-shaped curve for the E oscillators defined in Remark 3 and assume that the left and right branches of $\mathscr{C}_{s_J}$ can be written as $v_i = \Phi_L(w_i, s_J)$ and $v_i = \Phi_R(w_i, s_J)$, respectively. Assume that the left knee of $\mathscr{C}_{s_J}$ is at $w = w_L(s_J)$

for each s_J. We assume that the w-nullcline $\{g(v, w) = 0\}$ intersects each $\mathscr{C}_{s_J}$ along its left branch. From the first two equations in (2.6), this implies that the E oscillators are excitable for constant levels of synaptic input s_J. Suppose that this point of intersection of nullclines occurs at $w = w_F(s_J)$.

Remark 6. Note that if $\partial f/\partial w > 0$ and $\partial g/\partial v < 0$ near $\mathscr{C}_{s_J}$, then both $w_L(s_J)$ and $w_F(s_J)$ are increasing functions of s_J. This follows, since s_J represents inhibitory input, from implicit differentiation of the equations $f(\Phi_L(w_L(s_J), s_J), w_L(s_J)) - g_{inh}s_J(\Phi_L(w_L(s_J), s_J) - v_{inh}) = 0$ and $g(\Phi_L(w_F(s_J), s_J), w_F(s_J)) = 0$.

We can obtain reduced equations for the slow variables corresponding to each E oscillator as follows. First suppose that the E oscillator is silent. If the J oscillator is also silent, then the slow variables corresponding to the E oscillator are (w_i, s_J). This can be seen from (2.6)-(2.7) after rescaling in terms of the slow time variable $\tau = \epsilon t$ and then setting $\epsilon = 0$. While in the silent phase, the E oscillator lies on the left branch of $\mathscr{C}_{s_J}$; that is, $v_i = \Phi_L(w_i, s_J)$. Hence, if we let $G_L(w, s_J) = g(\Phi_L(w, s_J), w)$, then the slow variables satisfy

$$\begin{aligned} \dot{w}_i &= G_L(w_i, s_J) \\ \dot{s}_J &= -K_J s_J. \end{aligned} \tag{3.1}$$

Note that if the J oscillator is active then $s_J \equiv 1$. In this case, w_i is the only slow variable and it satisfies

$$\dot{w}_i = G_L(w_i, 1). \tag{3.2}$$

In a similar manner, we can derive a reduced equation for the evolution of E oscillators while they are active. Let $G_R(w, s_J) = g(\Phi_R(w, s_J), w)$. We will only consider solutions in which the J oscillator is active whenever an E oscillator is active. Hence, $s_J = 1$ and w_i satisfies the reduced equation

$$\dot{w}_i = G_R(w, 1). \tag{3.3}$$

We assume that the right knee of $\mathscr{C}_1$ is at $w = w_{RK}$. This is where the E oscillators jump down from the active phase. In the clustered solutions that we will consider, all E slow dynamics occur in the (w, s_J) phase space bounded by the curves displayed in Figure 4. We assume that $w_{RK} < w_L(0) < w_F(1)$, as shown, throughout the paper.

Finally, we consider the J oscillator. Let $\mathscr{C}^J_{s_{tot}}$ denote the cubic shaped curve $\{(v_J, w_J) : f_J(v_J, w_J) - g_{exc}s_{tot}(v_J - v_{exc}) = 0\}$. Assume that the left and right branches can be written as $v_J = \Phi^J_L(w_J, s_{tot})$ and $v_J = \Phi^J_R(w_J, s_{tot})$, respectively, and the left and right knees can be written as $w_J = w^J_L(s_{tot})$ and $w_J = w^J_R(s_{tot})$. We assume that the w_J-nullcline intersects each $\mathscr{C}^J_{s_{tot}}$ along its left branch and this point of intersection is at $w_J = w^J_F(s_{tot})$. Note that each s_i, and therefore s_{tot}, changes on the fast time scale. Hence, the only slow variable corresponding to the J oscillator is w_J. If $G^J_\kappa(w_J, s_{tot}) \equiv g_J(\Phi^J_\kappa(w_J, s_{tot}), s_{tot})$ for $\kappa = L, R$, then w_J satisfies the slow equation
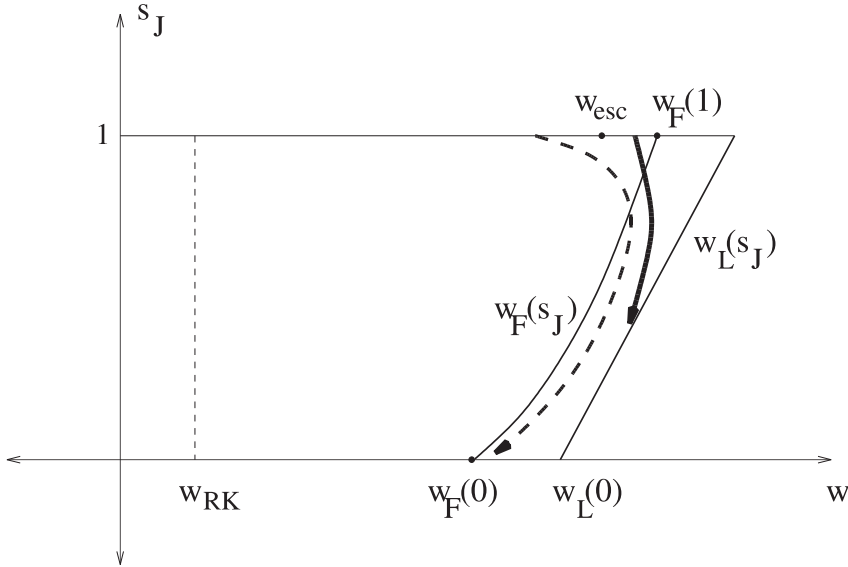
Fig. 4. The region in (w, s_J) phase space relevant for the E dynamics. The heavy solid line shows an example trajectory for large K_J, such that jump-up occurs. The dashed line shows an example for small K_J, such that jump-up does not occur. As indicated in Section 3.3, it takes time τ_{esc} for a solution of (3.2) with initial condition $w = w_{RK}$ to reach w_{esc}.

$$\dot{w}_J = G^J_\kappa(w_J, s_{tot}). \tag{3.4}$$

Remark 7. The reduced systems are very useful in analyzing the behavior of the E oscillators while they are silent. For example, one important issue will be whether each E oscillator is able to reach the jump-up curve after the J oscillator jumps down and releases the E oscillators from inhibition. When the J oscillator jumps down, $s_J = 1$. Hence, we need to determine for which values of w_0 the solution of (3.1) beginning at $(w_i, s_J) = (w_0, 1)$ reaches the jump-up curve. Note that solutions reach the curve for large K_J and $w_0 > w_L(0)$; that is, if K_J is sufficiently large, then the solution of (3.1) is nearly vertical as shown in Figure 4. Thus, for any K_J sufficiently large, there exists a corresponding $w_{esc} < w_F(1)$ such that the solution of (3.1) beginning at $(w_0, 1)$ will reach the jump-up curve for precisely those $w_0 \geq w_{esc}$. Note that if K_J is too small, then "escape" is never possible for any w_0. This is because the solution of (3.1) beginning at $(w_0, 1)$ will track close to the curve $w = w_F(s_J)$, as shown in Figure 4.

Numerical examples of clustered solutions in a globally inhibitory network with indirect inhibition, with two and three clusters in a population of 12 E oscillators, are shown in Figures 5–6. For these figures, each E and J oscillator was modeled with Hodgkin-Huxley type equations, with a leak current and a T-type calcium current; interested readers should see [5], [11], [13] for details. To switch between two and three clusters, we decreased θ_{inh}, increased ϵ, and decreased K_J (with a net increase in ϵK_J) in (2.7).
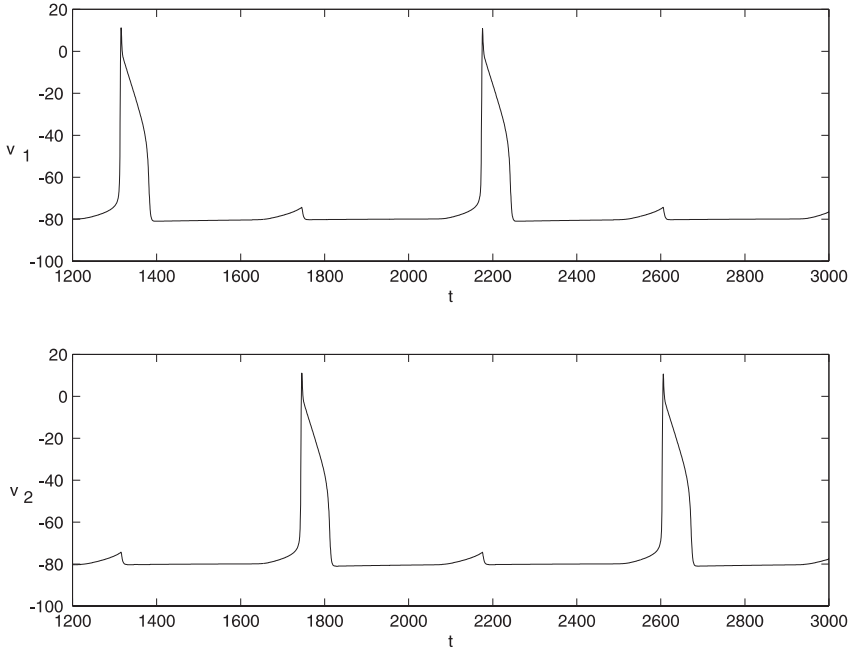
Fig. 5. Numerical example of a 2-cluster solution in a globally inhibitory network with 12 E oscillators. Each subplot shows the evolution of v versus t for a different cluster as the two clusters alternate firing. This and other numerical figures were generated using XPPAUT, developed by G.B. Ermentrout.

Figure 7 shows a numerical example of a segment of an E oscillator trajectory in (w, s_J) space during the 2-cluster oscillation of Figure 5. The segment shown starts with $s_J \approx 1$ and s_J beginning to decay; the slow variable w begins to decrease when the trajectory crosses the fixed point curve $w_F(s_J)$. The oscillator fires when it hits the jump-up curve $w_L(s_J)$; this corresponds to one of the sharp increases in v seen in Figure 5, but the increase in v does not show up in the projection to (w, s_J) space. After this, the oscillator is in the active phase, and hence on the right branch of $\mathscr{C}_{s_J}$, where w continues to decrease. This is why the trajectory in Figure 7 appears to cross through the jump-up curve. Soon after the firing, inhibition resumes, and s_J jumps up to near 1 while w continues to decrease since the E oscillator is active. When the oscillator reaches the right knee w_{RK}, it falls back down to the silent phase and evolves with $s_J = 1$ and increasing w until J falls down (not shown).

Figure 8 shows a numerical example with trajectories from two different E oscillator clusters in the 3-cluster oscillation of Figure 6, one of which (dashed line) fires during the time shown and one of which (dash-dotted line) does not. Along the parts labeled '1', inhibition decays, while along '2', inhibition resumes. After the period shown, the oscillators evolve, one in the active phase and one in the silent phase, with $s_J \approx 1$, such that the projections of their trajectories to (w, s_J) space cross (not shown).
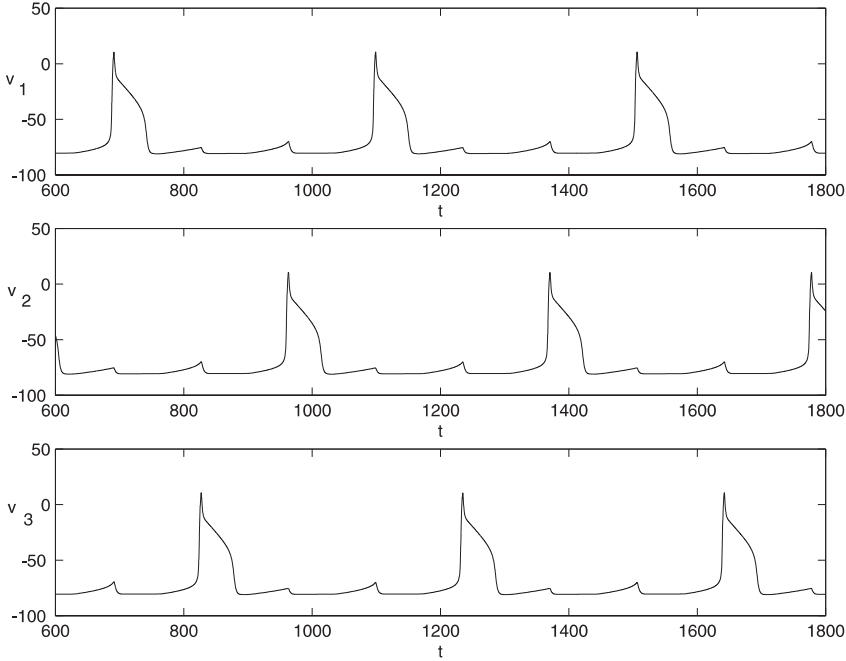
Fig. 6. Numerical example of a 3-cluster solution in a globally inhibitory network with 12 E oscillators.

3.3. Statement of the main result

In this subsection, we state our main result concerning the existence and stability of clustered solutions in a globally inhibitory network with a population of N excitable E oscillators. To clarify the presentation and notation, we make some simplifying assumptions. A more general analysis, with less restrictive assumptions, is given in Section 3.6. We begin by introducing some additional notation; these denote the durations of various stages of the oscillation, namely silent and active phase lengths for the different oscillator populations and the length of time during which inhibition decays. Theorem 1 will give precise conditions for when a particular clustered solution exists in terms of these times. We note that these times can in turn be directly related to parameters in a particular model. This is discussed in more detail in Remark 9, in the discussion following Corollary 1, and in Section 4.

Let τ_E and τ_J denote the durations of the E and J active phases, respectively. These actually depend on several factors including where the jumps up and down take place and which right branch an oscillator lies on; however, we assume here that both τ_E and τ_J are constant. In Section 3.6, we demonstrate that one can easily obtain bounds on the sizes of τ_E and τ_J; these bounds allow us to generalize the theorem which follows.

Let w_{esc} be as defined in Remark 7 and shown in Figure 4. That is, the solution of (3.1) beginning at $(w_0, 1)$ will reach the jump-up curve if and only if $w_0 \geq w_{esc}$. We denote by τ_S the time it takes for this solution to reach the jump-up curve (e.g.,
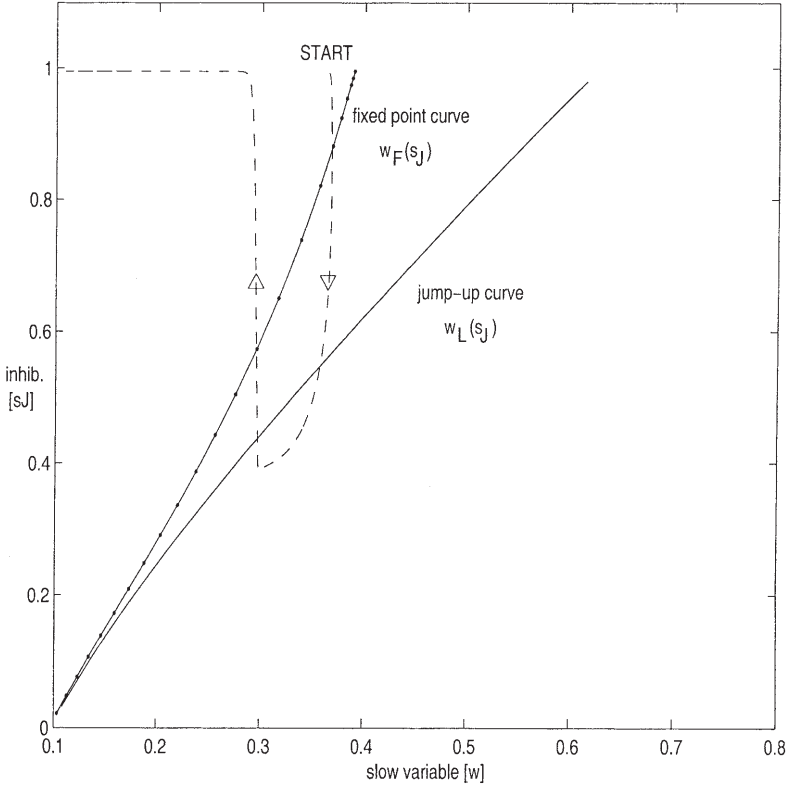
Fig. 7. A single E trajectory in a 2-cluster solution, projected to the phase space of the slow variable (w) and inhibition (s_J). The oscillator evolves from the point labeled START as its inhibition gradually decays; arrowheads show direction of evolution. Once it crosses the jump-up curve, it is in the active phase.

the duration of the solid line in Figure 4 for large K_J). Note that τ_S depends on the initial position w_0; however, we ignore this dependence in this section. Otherwise, we could state our results in terms of minimum and maximum times $\bar{\tau}_S$ and $\underline{\tau}_S$; this is done in Section 3.6 below. Note that $w_{esc} \to w_L(0)$ and $\tau_S \to 0$ as $K_J \to \infty$. Let τ_{esc} be the time for the solution of (3.2) with initial condition $w = w_{RK}$ to reach w_{esc}.

We next need an assumption that implies that the J oscillator jumps up if it receives excitation from a sufficiently large number of E oscillators. It is possible that just a few E oscillators is not enough to excite the J oscillator to fire. The J oscillator will be able to jump up upon receiving excitation of strength S only if the left knee of the cubic $\mathscr{C}_S^J$ lies below the point $w_J = w_F^J(0)$. From (2.8), if m E oscillators are active, then $s_{tot} = \frac{m}{N} s_A$. Therefore, we assume that there exists M such that if $m \geq M$, then

$$w_L^J\left(\frac{m}{N} s_A\right) < w_F^J(0) \tag{3.5}$$
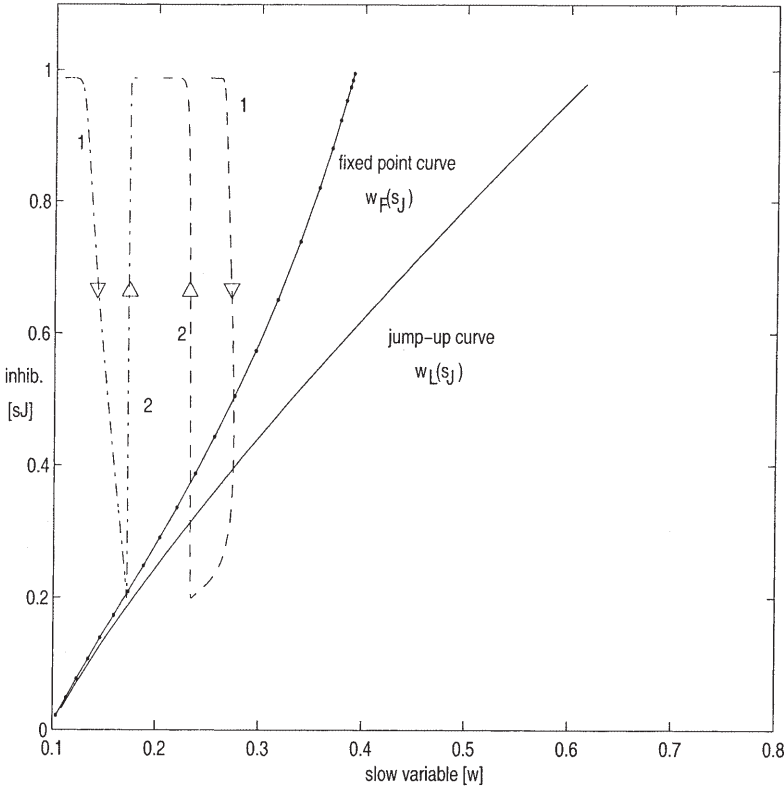
Fig. 8. Projection of E trajectories from two different E clusters in a 3-cluster solution. Arrowheads show directions of evolution. After a decay of inhibition ('1'), one oscillator shown (dashed trajectory) hits the jump-up curve and fires while the other one (dash-dotted trajectory) does not jump up before inhibition resumes ('2').

Finally, we define a time length that is related to the time the J oscillator spends recovering in the silent phase. Since we are assuming that the J oscillator is active for longer than the E cluster, the J oscillator jumps down at the right knee of the $s_{tot} = 0$ cubic; that is, at $w_J = w_R^J(0)$. After this, w_J satisfies (3.4) with $\kappa = L$ and $s_{tot} = 0$ as long as the J oscillator is silent. Let $\tau_R(M)$ be the time for the solution of (3.4) with $\kappa = L$ and $s_{tot} = 0$, starting at $w_R^J(0)$, to reach $w_L^J(\frac{M}{N} s_A)$. Together with the discussion in the previous paragraph, it then follows that if the J oscillator spends more than time τ_R in the silent phase, and if at least M E oscillators then jump up, then the J oscillator will also jump up in response to the E cluster firing.

Recall that in Section 3.2, we assumed that $w_{RK} < w_L(0) < w_F(1)$. The first inequality implies that when an E oscillator jumps down, it does so below the left knee of C_0. The second inequality is motivated by the discussion in Remark 7; it is needed to guarantee that E oscillators are able to reach the jump up curve once they are released from inhibition. Under this structural assumption, the following theorem holds.

Theorem 1. *Fix N. Assume there exists M such that (3.5) holds for all $m \geq M$ and assume that $\tau_E < \tau_J$. Let n be the unique positive integer such that both of the following hold:*

$$i) \ n\tau_J - \tau_E + (n-1)\,\tau_S > \tau_{esc}$$
$$ii) \ (n-1)\tau_J - \tau_E + (n-2)\,\tau_S < \tau_{esc}$$

If $n \leq \frac{N}{M}$, $\tau_R(M) < \tau_S$, and K_J is sufficiently large, then there exists an n-cluster periodic solution of (2.6), (2.7) such that each E cluster contains at least M oscillators. This solution is stable, for K_J sufficiently large, if $|G_L(w, s_J)| < |G_R(w, 1)|$ for $w_L(0) < w < w_F(1)$.

Remark 8. The assumption $\tau_E < \tau_J$ was discussed earlier in Section 3.1. It is needed so that E oscillators are able to recover sufficiently in their silent phase before the J oscillator jumps down and releases them from inhibition. As discussed in Remark 7, we need to assume that K_J is sufficiently large so that when E oscillators are released from inhibition, they are capable of reaching the jump-up curve. The assumption $\tau_R < \tau_S$ is needed so that the J oscillator is able to recover sufficiently in its silent phase before a cluster of E oscillators jump up.

Remark 9. Parameters appearing in specific globally inhibitory networks of the form (2.6)-(2.7) affect the times $\tau_E, \tau_J, \tau_R, \tau_S$ in clearly traceable ways. For example, the main effect of strengthening the low-threshold calcium conductance of thalamocortical relay cells, whose burst behavior can be described by (2.6), is a lowering of the right knee for E. This lengthens the relay active phase and increases τ_E. Other examples of such effects, specifically related to the period of oscillations, are explored following Corollary 1 in the next subsection.

Remark 10. The stability condition $|G_L(w, s_J)| < |G_R(w, 1)|$ implies that the rate at which the slow variable w_i evolves just before an E oscillator jumps up is slower than the rate w_i evolves just afterwards. This condition is very similar to that needed in [15] in their discussion of *Fast Threshold Modulation* (FTM); see Remark 13 in Section 3.5. One expects this condition to be satisfied in general, because E_i jump up when they reach the curve $w_L(s_J)$, typically close to $w_F(s_J)$, where $G_L(w_F(s_J), s_J) = 0$.

Remark 11. Condition (i) maintains the oscillation, while condition (ii) prevents each cluster from catching up to the one ahead of it.

Remark 12. If $n = 1$, then condition (i) becomes $\tau_J > \tau_E + \tau_{esc}$. This is exactly the condition derived in [13] for the existence of a synchronous solution. Here, condition (ii) is not relevant. For the 2-cluster case, conditions (i), (ii) reduce to $\tau_J - \tau_E < \tau_{esc} < 2\tau_J - \tau_E + \tau_S$. In the limit of fast inhibitory decay, $\tau_S \to 0$ and the condition becomes $\frac{1}{2}(\tau_E + \tau_{esc}) < \tau_J < \tau_E + \tau_{esc}$, which was also derived in [13].

3.4. Existence of the clustered solution

Here we prove that the globally inhibitory network exhibits an n-cluster solution if the hypotheses of Theorem 1 are satisfied. We consider $n \geq 3$; the case of $n = 2$ is analogous but simpler and hence we omit details. We first assume that n divides N and seek a solution for which each of the clusters consists of exactly N/n members. In this case the analysis is identical to the consideration of a population of n E oscillators with each oscillator representing its own cluster.

Suppose the network starts with J active and with each E cluster in the silent phase, on the left branch of the $s_J = 1$ nullcline $\mathscr{C}_1$. Label the E clusters as $1, \ldots, n$ with $w_i < w_{i+1}$ for $i = 1, \ldots, n-1$. Further, assume that cluster 1 is initially at $(w_{RK}, 1)$, the position it would have if it had just jumped down from the active phase. In this configuration, cluster n will be the next to fire; a change in the cluster ordering cannot occur for K_J large relative to the rate of change of w in the silent phase.

We measure distance between adjacent clusters along the left branch of $\mathscr{C}_1$ in terms of a time metric (e.g. [8], [15], [21]). In this metric, the statement that two clusters lie a distance T apart at time τ means that the trailing cluster will reach the current position of the lead cluster after time T. This measurement is meaningful if we measure at times when all E clusters are in the silent phase but J is active, such that $s_J = 1$. Then all E clusters lie on the same trajectory in (w, s_J) phase space, given by (3.2). Hence, for large K_J, such that each w_i changes little during the interludes of inhibitory decay, the distance between clusters remains invariant to leading order as long as they are in the silent phase.

Let $\tau_{esc}^- = \tau_{esc} - (\tau_J - \tau_E)$, which is positive by condition (ii). We then define $a = \tau_{esc}^-/(n-1)$ and $b = \tau_{esc}^-/(n-2)$. To prove the existence part of Theorem 1, we assume that the distance between each pair of adjacent clusters is initially within the interval (a, b). We then prove that this assumption is still satisfied at the moment of each subsequent E cluster fall-down. Moreover, the clusters take turns firing, along with the J oscillator (since $\tau_R(M) < \tau_S$), in such a way that no two clusters are ever simultaneously active. This yields a fixed point which is the desired n-cluster periodic solution.

Assume that when $\tau = 0$, the clusters are lined up on the left branch of $\mathscr{C}_1$ as described above; in particular, the distance between adjacent clusters is within the interval (a, b). One thing we need to prove, which is shown below, is that cluster n will then be able to reach the jump up curve and fire. If this is the case, then choose T to be the time when cluster n jumps down again. We must also prove that no other cluster fired in the interval $\tau \in [0, T]$; moreover, when $\tau = T$, the distance between each pair of adjacent clusters lies within (a, b).

Suppose, for the moment, that cluster n does indeed jump up and it is the only cluster to do so for $\tau \in [0, T]$. The distance between the other clusters remains invariant, so it is obvious that when $\tau = T$, the distance between cluster i and cluster $i+1$, for $i = 1, 2, .., n-2$ lies within (a, b). We must still show that the distance between cluster n and cluster 1 lies within (a, b). Since $w_1(0) = w_n(T) = w_{RK}$, this is equivalent to showing that $T \in (a, b)$. From the definitions, cluster n fires after time $\tau_J - \tau_E + \tau_S$ and the time it spends in the active phase is τ_E. Hence,

$T = \tau_J + \tau_S$. Then $T \in (a, b)$ follows from the definitions and conditions (i) and (ii).

We next show that cluster n must, in fact, reach the jump up curve and fire. Since the time between each adjacent cluster is initially greater than $a = \tau_{esc}^-/(n-1)$, it follows that the time between $w_{RK} = w_1(0)$ and w_n is initially greater than $(n-1)a = \tau_{esc}^- = \tau_{esc} - (\tau_J - \tau_E)$. Now, J jumps down when $\tau = \tau_J - \tau_E$. Hence, when J jumps down, the time from w_{RK} to w_n is greater than τ_{esc}, so, from the definitions, $w_n > w_{esc}$. This is exactly what is needed to guarantee that cluster n is able to reach the jump-up curve. A similar argument shows that when J jumps down, E cluster $n-1$ has $w_{n-1} < w_{esc}$, so cluster $n-1$ cannot jump up during this cycle.

In the preceding proof, we assumed that n divides N; however, the proof also holds if this last condition is not satisfied. Since $n \leq N/M$ we may assume that each of the n clusters has at least M oscillators. We then proceed as before. The primary difference in the analysis is that the input that the J oscillator receives depends on which cluster is active. Hence, the J oscillator will lie on different right branches in its active phase, depending on which cluster of E oscillators it receives input from. However, we are currently assuming that the time the J oscillator spends in its active phase is constant; in particular, τ_J does not depend on the level of input the J oscillator receives. For this reason, no change in the proof of the theorem is needed. In Section 3.6, we will discuss what modifications to Theorem 1 are needed if τ_J is no longer assumed to be constant. This will clarify how changing the number of oscillators per cluster affects the analysis.

Corollary 1. *When an n-cluster solution exists, it has period $\mathcal{T}_n$ given by $\mathcal{T}_n = n(\tau_J + \tau_S)$*

This follows immediately from the construction of the n-cluster solution. Each oscillation can be decomposed into a part of duration τ_J when J is active and a part of duration τ_S when inhibition decays. Thus, the influence of parameters on period follows directly from their influence on these durations.

Figures 9–10 show several examples of the effects of parameters on period in the 3-cluster oscillation of Figure 6. The most obvious of these in Figure 9 is the dashed curve, which shows the decrease in period with increase in K_J, the inhibitory decay rate, in (2.7); this clearly decreases τ_S. In our simulations, we take $g(v_i, w_i) = \phi(w_\infty(v_i) - w_i)/\tau(v_i)$ in (2.6). The solid curve in Figure 9 represents the effect of varying ϕ. This variation affects τ_E, which has little effect on period; however, increasing this rate influences period slightly by moving the E_i farther along in the silent phase with $s_J = 1$, such that they can fire with less decay of s_J and thus smaller τ_S. The other two curves show the effects of increasing parameters in (2.6) that raise the curve of knees in the silent phase, thereby slightly increasing τ_S and thus slightly increasing the period. One of these parameters is g_{inh}, which corresponds to the strength of inhibitory coupling to the E (the other is the leak current conductance for the E). Thus, we see the surprising effect, also seen in the context of synchronous solutions in [5], [13], that increasing the strength of
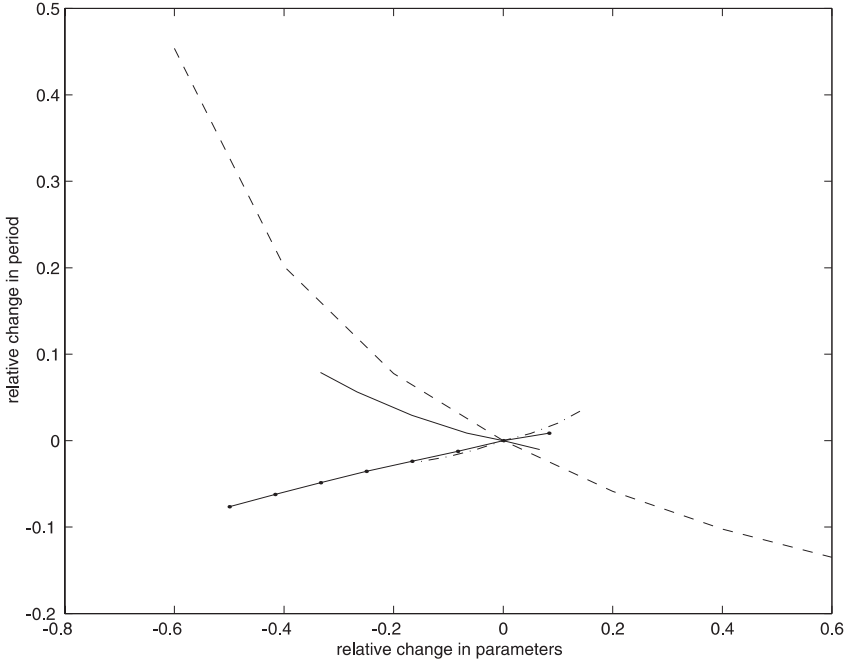
Fig. 9. Relative change in period of a clustered solution as parameters relevant to dynamics of the E oscillators vary. Parameters were started at fixed initial values and period was measured. Relative refers to the ratio of the size of change to the initial value. Dashed curve: K_J in (2.7) was varied. Solid curve: the time constant of $g(v_i, w_i)$ in (2.6) was varied. Solid-dotted curve: g_{inh} in (2.6) was varied. Dash-dotted curve: a parameter in $f(v_i, w_i)$ in (2.6) was varied, raising the left knee of $f = 0$.

inhibition has little effect on period, and the effect that it does have is to lengthen the period of the oscillations.

Figure 10 shows some analogous results for parameters that affect, or might be expected to affect, times associated with J. The relatively steep curves show the effects of increasing the parameter ϕ_J in the equation $w'_J = \phi_J(w_{J_\infty}(v) - w_J)/\tau_J(v)$ in (2.7) and of raising the cubics for J (by increasing its leak current conductance), which both decrease τ_J and hence the period. The solid curve displays the additional surprising fact that changes in the strength of excitation to J, namely g_{exc} in (2.7), have little effect on period. This follows from a different mechanism than the invariance of period with respect to changes in inhibitory strength, since τ_J, unlike τ_E, strongly influences period. The insensitivity of period to g_{exc} occurs primarily because the J active phase is longer than the E active phase, such that J always returns to the $s_{tot} = 0$ cubic in the active phase before jumping down, no matter how excited J is while the E are active.

The role of parameters in determining the period of clustered oscillations can also be seen directly via the approach of Section 4. This approach leads to the period formula for a 2-cluster solution in Corollary 2, the utility of which is explored in the discussion which follows its statement in Section 4.1 below.
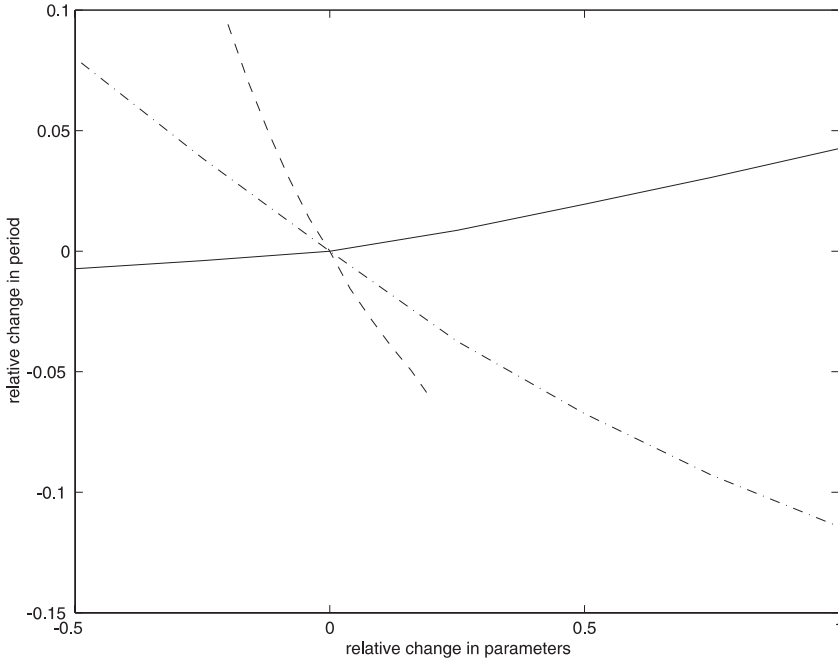
Fig. 10. Relative change in period of a clustered solution as parameters relevant to J dynamics vary. Dashed curve: the time constant of $g_J(v_J, w_J)$ in (2.7) was varied. Solid curve: g_{exc} in (2.7) was varied. Dash-dotted curve: a parameter in $f_J(v_J, w_J)$ in (2.7) was varied.

3.5. Stability of clustered solutions

There are two issues related to the stability of the clustered solutions. The analysis in the proof of existence in the previous subsection shows that oscillators within different clusters remain separated from each other; in particular, they can never lie in the active phase at the same time. We must also prove that if the oscillators within a cluster are perturbed slightly from their trajectories in phase space, then they are compressed back towards each other under the subsequent flow.

We now consider initial conditions in which the positions of the oscillators within each cluster are close, but not necessarily equal, to each other. We also take the inhibition to be indirect, since the solution cannot be stable if the synapses are direct (see [12], [13]). The instability with direct synapses follows because if two E oscillators E_1, E_2 start from slightly different positions in the silent phase and E_1 jumps up, then J may immediately jump up. Direct inhibition will then instantly (with respect to the slow time scale) make $s_J = 1$. Thus, E_2 will instantly jump back to the left branch of $\mathscr{C}_1$ away from its firing threshold, breaking up the cluster and hence destabilizing the clustered solution. Indirect synapses, on the other hand, induce a lag between the firing of one E oscillator and the onset of inhibition, providing a window of opportunity for other E oscillators to fire.

To establish stability within clusters with indirect inhibition requires showing that oscillators that start close together in phase space are brought closer together as

they evolve. This can be understood by again measuring distance in a time metric, or more specifically a time metric corresponding to the w-coordinate, call it ρ_w. We can define the distance between two oscillators in the silent phase in the metric ρ_w as a function of inhibition s_J. This is done, for fixed s_J, by letting the time measurement between the oscillators equal the time for the oscillator with smaller w value to evolve to the position of the other oscillator under the first equation of (3.1). In a similar manner, we define the metric ρ_w while the oscillators are in the active phase. With this definition, under the hypothesis that $|G_L(w, s_J)| < |G_R(w, 1)|$ for $w_L(0) < w < w_F(1)$ (given in Theorem 1), it is easy to show that ρ_w decreases when oscillators in the same cluster jump up. That is, after the oscillators jump up, the faster flow that they experience causes the same difference between their w coordinates to correspond to a shorter time lag between them. There is no change in ρ_w over the jump down since, for a small perturbation from the state of complete synchrony within the cluster, all oscillators in a cluster jump down from the right knee w_{RK}. Thus, the time by which one oscillator lags another in the active phase remains the time by which it lags the other just after they reach the silent phase.

The metric ρ_w is invariant for most of the time that the oscillators are actually in the silent and active phases, since they evolve under the first equation of (3.1) with the same s_J in most of the silent phase and under (3.3) in the active phase. The only exception occurs during the interludes in the silent phase when s_J decreases from 1; for K_J large, these affect ρ_w only negligibly. Thus, the hypotheses of Theorem 1 yield stability within clusters.

Remark 13. The compression mechanisms responsible for the stability of the synchronous solution [13] and the stability of oscillators within a cluster for a clustered solution are very similar. In fact, this compression mechanism is also similar to the compression mechanism in Fast Threshold Modulation [8], [15], [21]. In each of these scenarios, the oscillators undergo fast jumps between slow phase spaces and the slow variable, w, evolves slower before the jump up than after. This produces compression in a time metric. What distinguishes these situations is the mechanism that allows them to jump up. In FTM, one oscillator reaches the jump-up point at a knee, so that it can *escape* from the silent phase. This, in turn, lowers the other oscillators' nullclines so that they are forced to jump up. For the synchronous solution in globally inhibitory networks, all the E oscillators jump up after J falls down and *releases* them from inhibition. In a clustered solution, the oscillators in the silent phase cannot fire until another cluster jumps down. The J must then still jump down before a new E cluster is released from inhibition.

Remark 14. In terms of Euclidean distance, there is exponential compression of trajectories near $w_F(1)$; if τ_J is sufficiently long, such that E oscillators spend a long time in the silent phase, then this easily dominates any possible expansion over the remainder of the oscillators' trajectories. Of course, if τ_J were extremely long, then synchrony of the E oscillators would result [13].

3.6. Less restrictive assumptions; 2-cluster case

In the preceding subsections, we simplified the analysis by assuming that the time durations τ_E, τ_J, and τ_S are constant. This amounts to assuming that each E cluster

active phase has the same duration, each J active phase has the same duration, and the time from J jump-down to the next E firing is constant; that is, we restricted the class of clustered solutions under consideration. Here we demonstrate how one can generalize Theorem 1 if these assumptions are no longer satisfied. We first obtain upper and lower bounds for each of the time durations and then derive conditions similar to those in Theorem 1 for when a particular clustered solution exists. Here, we only consider the case of a solution consisting of two equal sized clusters of E oscillators in detail.

We obtain bounds on the active phase of each E oscillator as follows. Each E oscillator jumps up at some value of w that satisfies $w_L(0) < w < w_F(1)$ and jumps down at $w = w_{RK}$. Let $\underline{\tau}_E$ be the time for the solution of (3.3) beginning at $w_L(0)$ to reach w_{RK} and let $\bar{\tau}_E$ be the time for the solution of (3.3) beginning at $w_F(1)$ to reach w_{RK}. Then the length of each E oscillator's active phase is bounded from below by $\underline{\tau}_E$ and bounded from above by $\bar{\tau}_E$.

In a similar way we obtain a bound for the J oscillator's active phase. The J oscillator jumps up at some w_J that satisfies $w_L^J(\frac{s_A}{2}) < w_J < w_F^J(0)$ and jumps down at $w_J = w_R^J(0)$. Let $\underline{\tau}_J$ be the time for the solution of (3.4), beginning at $w_L^J(\frac{s_A}{2})$ with $s_{tot} = s_A/2$ and switching to $s_{tot} = 0$ after time $\bar{\tau}_E$, to reach $w_R^J(0)$ and let $\bar{\tau}_J$ be the time for the solution of (3.4), beginning at $w_F^J(0)$ with $s_{tot} = s_A/2$ and switching to $s_{tot} = 0$ after time $\underline{\tau}_E$, to reach $w_R^J(0)$. Then the length of the J oscillator's active phase is bounded by $\underline{\tau}_J$ and $\bar{\tau}_J$.

We next obtain a bound for τ_S; this is the time required for the synapse to recover sufficiently after the J oscillator jumps down before an E oscillator can reach the jump up curve and fire. Let w_{esc} and τ_{esc} be as before. Recall that an E oscillator can fire if and only if its w coordinate lies in the interval $[w_{esc}, w_F(1))$ when the J oscillator jumps down. Let $\bar{\tau}_S$ be the time for the solution of (3.1) beginning at $(w_{esc}, 1)$ to reach the jump up curve and let $\underline{\tau}_S$ be the time for the solution of (3.1) beginning at $(w_F(1), 1)$ to reach the jump up curve. Since $w_{esc} < w_F(1)$, it follows that $\underline{\tau}_S < \tau_S < \bar{\tau}_S$.

As in the preceding section we assume that $w_{RK} < w_L(0) < w_F(1)$. We need to also assume that if one cluster of E cells fire, then the J oscillator also fires. If there are just two clusters, the total input the J oscillator receives is $s_{tot} = s_A/2$. Therefore, we assume that $w_L^J(s_A/2) < w_F^J(0)$. Using the notation of the preceding section, this implies that we can take $M = N/2$. We let τ_R be the recovery time of J in the silent phase, as in the preceding section with this choice of M.

We can now state the following theorem. This gives precise conditions for when there exists a 2-clustered solution.

Theorem 2. *If K_J is sufficiently large then a 2-cluster singular periodic solution exists, if each of the following three conditions are satisfied:*
  (C1) $\bar{\tau}_E < \underline{\tau}_J$
  (C2) $\bar{\tau}_J - \underline{\tau}_E < \tau_{esc} < \underline{\tau}_J$
  (C3) $\tau_R < \underline{\tau}_S$
This solution is stable, for K_J sufficiently large, if $|G_L(w, s_J)| < |G_R(w, 1)|$ for $w_L(0) < w < w_F(1)$.

This theorem is proved just as the previous one so we do not give the details. The condition (C1) is needed to ensure that the E active phase is shorter than the J active phase. The first inequality in (C2) ensures that the trailing E cluster flows to have its $w > w_{esc}$ while J is active. The trailing cluster will then be able to reach the jump-up curve and fire once inhibition decays sufficiently. The second inequality in (C2) ensures that after the leading E cluster jumps down, its w value does not reach w_{esc} while J is still active. Hence, this leading cluster will not be able to reach the jump-up curve and fire together with the trailing cluster. Finally, (C3) is needed for the same reason as in Theorem 1; it ensures that the J oscillator is sufficiently recovered when each E cluster jumps up. Hence, the J oscillator can jump up in response to the firing E cluster, as needed to sustain the oscillation.

4. A more explicit map approach

In Section 3, we derived sufficient conditions for existence and stability of clustered solutions, stated in terms of times for various phases in an oscillatory cycle. In this section, as earlier, we consider clustered states as fixed points of maps; however, we now make certain simplifications which allow us to write down the maps more explicitly. This leads to fixed point equations for which we can show the existence of solutions, together with precise stability conditions and a period formula. These are given in terms of parameters in the equations and positions of certain key structures in phase space, such as the positions of left and right knees. These conditions are particularly useful in that they explicitly reveal the roles of these parameters and structures in forming clustered solutions. We begin with consideration of a mutually coupled network, since the conditions can be stated most cleanly in that setting. Globally inhibitory networks are considered in Section 4.2.

4.1. 2-cluster solutions in a mutually coupled network

To begin, we consider the case of a population of 2 mutually coupled oscillators with direct inhibitory coupling. We focus on a periodic solution in which the oscillators fire alternately, with a relative phase shift given by half the period of the oscillation, as shown in Figure 11. This was generated using a model with Hodgkin-Huxley type equations, with a leak and T-type calcium current for each cell, as used in the globally inhibitory figures [5], [11], [13].

We refer to this solution as an *antisynchronous* state. Set $s_{tot} = s_1 + s_2$ where each s_i satisfies (2.4). Note that $s_{tot} = 1/2$ while one of the oscillators is active. The active oscillator will jump down at w_{RK}, the position of the right knee of the $s_{tot} = 1/2$ cubic. As before (e.g. Figure 4), let $w_F(s_{tot})$ denote the curve of critical points and let $w_L(s_{tot})$ denote the jump-up curve in slow (w, s_{tot}) phase space. We let $w^* = w_F(1/2)$.

We assume that $g(v, w) = \phi_S(w^* - w)$ in the silent phase and $g(v, w) = -\phi_A w$ in the active phase. Here, ϕ_S and ϕ_A are constants. The form of g in the silent phase derives from the fact that v is approximately constant on the left branch of the $s_{tot} = 1/2$ cubic in the models of interest, which typically have $g(v, w) = (w_\infty(v) - w)/\tau(v)$ for a sigmoid, monotone decreasing function $w_\infty(v)$. Further,
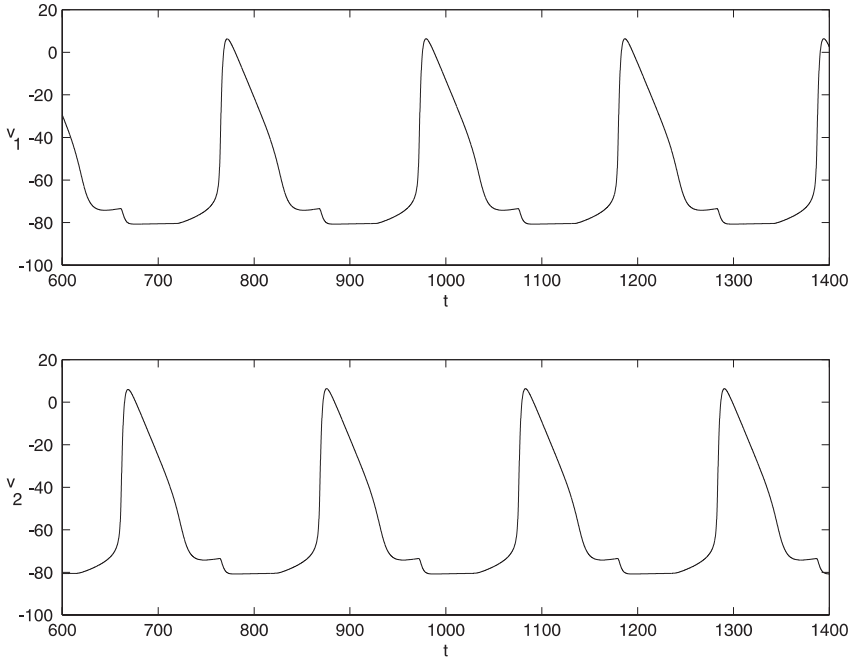
Fig. 11. Numerical example of an antisynchronous 2-cluster solution for a mutually coupled network.

in an excitable regime, the intersection of $w_\infty(v)$ with each cubic v-nullcline yields $w_F(s_{tot})$. The form of g in the active phase is also based on these models, since $w_\infty(v) \approx 0$ and $\tau(v) \approx \tau_A$, a constant, in the active phase.

Under these assumptions, plus the assumption that K is sufficiently large, we next derive a map which has the antisynchronous solution as a fixed point. The assumption of sufficiently large K allows us to approximate $g(v, w)$ by $\phi_S(w^* - w)$ even for $s_{tot} < 1/2$ in the silent phase and to ignore the fact that trajectories must cross the curve $w_F(s_{tot})$ to reach $w_L(s_{tot})$.

Consider the situation in which oscillator 1 has just fallen down from the active phase, so that $s_{tot} = 1/2$ and $w_1 = w_{RK}$, and oscillator 2 has initial coordinates $(w_0, 1/2)$ in the silent phase for some fixed constant w_0. Due to the nature of the coupling, s_1, s_2 subsequently decay via $\dot{s} = -Ks$. Let τ_s denote the time from $s_{tot} = 1/2$ until oscillator 2 reaches the curve of knees, say at $s_{tot} = s_k < 1/2$; then

$$\tau_s = \frac{1}{K} \ln \left(\frac{1}{2s_k} \right).$$

Let τ_a denote the amount of time that oscillator 2 is active after it jumps up. This is determined by the evolution of $\dot{w} = -\phi_A w$ with $w(0) = w_L(s_k)$ such that $w(\tau_a) = w_{RK} < w_L(s_K)$, so

$$\tau_a = \frac{1}{\phi_A} \ln \left(\frac{w_L(s_k)}{w_{RK}} \right).$$

A 1-dimensional map Π can be defined by inputing the initial w-value of oscillator 2, namely w_0, and outputting the w-value of oscillator 1 when oscillator 2 falls down. Then for sufficiently large K, $\Pi(w_0)$ is approximately given by the evolution of $\dot{w} = \phi_S(w^* - w)$, $w(0) = w_{RK}$ for a time $\tau_s + \tau_a$; that is,

$$\begin{aligned} \Pi(w_0) &= w^* + (w_{RK} - w^*)e^{-\phi_S(\tau_s+\tau_a)} \\ &= w^* + (w_{RK} - w^*)(2s_k)^{\phi_S/K} \left(\frac{w_{RK}}{w_L(s_k)} \right)^{\phi_S/\phi_A}. \end{aligned} \tag{4.1}$$

Note that s_k is defined implicitly as follows. The evolution of oscillator 2 in the silent phase for sufficiently large K is approximated by the initial value problem

$$\begin{aligned} \dot{w} &= \phi_S(w^* - w), \quad w(0) = w_0, \\ \dot{s} &= -Ks, \qquad\qquad s(0) = 1/2 \end{aligned} \tag{4.2}$$

until $\tau = \tau_s$, at which time $s = s_k$. The time τ_s is distinguished as the first time such that $w(\tau) = w_L(s(\tau))$. From (4.2) we thus obtain

$$w^* + (w_0 - w^*) \left(\frac{1}{2s_k} \right)^{\phi_S/K} = w_L(s_k), \tag{4.3}$$

which defines s_k.

With this definition, we can conclude the existence of a fixed point of Π, namely the desired symmetric antisynchronous solution, by using the fact that (4.1) yields the fixed point equation

$$w^* + (w_{RK} - w^*)(2s_k)^{\phi_S/K} \left(\frac{w_{RK}}{w_L(s_k)} \right)^{\phi_S/\phi_A} = w_0 \tag{4.4}$$

or

$$(2s_k)^{\phi_S/K} \left(\frac{w_{RK}}{w_L(s_k)} \right)^{\phi_S/\phi_A} = \frac{w_0 - w^*}{w_{RK} - w^*}, \tag{4.5}$$

where $s_k = s_k(w_0)$ from (4.3). At $w_0 = w_{RK}$, clearly $\frac{w_0-w^*}{w_{RK}-w^*} = 1 > (2s_k)^{\phi_S/K} \left(\frac{w_{RK}}{w_L(s_k)} \right)^{\phi_S/\phi_A}$, since $s_k < 1/2$ and $w_{RK} < w_L(s_k)$. Thus, (4.5) surely holds for some $w_0^* \in (w_{RK}, w^*)$ if

$$(2s_k(w^*))^{\phi_S/K} \left(\frac{w_{RK}}{w_L(s_k(w^*))} \right)^{\phi_S/\phi_A} > 0. \tag{4.6}$$

Since $s_k(w^*) = 1/2$ and $w_L(1/2) = w^*$, the left hand side of (4.6) is exactly $(w_{RK}/w^*)^{\phi_S/\phi_A}$, a positive number. This gives us the existence of a fixed point.

Remark 15. In the above existence proof, we implicitly assumed a trajectory of (4.2) with $w_0 = w_{RK}$ would reach $w_L(s)$. The same type of argument works otherwise as well. In that case, there exists some minimal w_0 value, w_{esc}, for which jump-up can occur, and at $w_0 = w_{esc}$, the right hand side of (4.5) exceeds the left hand side.

Proposition 1. *For fixed parameter values, with the simplified w-dynamics described above, the singular antisynchronous solution that forms a fixed point of Π is stable if and only if*

$$(2s_k)^{\phi_S/K} < w_L'(s_k) + 2(w^* - w_0^*)\left(\frac{\phi_S}{Ks_k}\right)(2s_k)^{\phi_S/K} \tag{4.7}$$

where $(w_L(s_k), s_k)$ is the point on $w_L(s_{tot})$ from which each oscillator jumps up.

Remark 16. In application, one might know the values of ϵK, $\epsilon\phi_S$ rather than K, ϕ_S. Since K and ϕ_S always appear as a ratio in 4.7, they can be replaced by ϵK and $\epsilon\phi_S$, respectively.

Proof. A necessary and sufficient condition for the stability of a fixed point w_0^* is $|\Pi'(w_0^*)| < 1$. A simple differentiation of (4.1) yields

$$\Pi'(w_0) =$$
$$(w_{RK} - w^*)(2s_k)^{\phi_S/K}\left(\frac{w_{RK}}{w_L(s_k)}\right)^{\phi_S/\phi_A}\left[\frac{\phi_S}{Ks_k} - \frac{\phi_S}{\phi_A}\frac{w_L'(s_k)}{w_L(s_k)}\right]\frac{\partial s_k}{\partial w_0}, \tag{4.8}$$

where implicit differentiation of (4.3) yields

$$\frac{\partial s_k}{\partial w_0} = \frac{(2s_k)^{\phi_S/K}}{w_L'(s_k) + (w^* - w_0)(2s_k)^{\phi_S/K}\frac{\phi_S}{Ks_k}}, \tag{4.9}$$

a positive quantity.

Let w_0^* denote a fixed point of Π which constitutes an antisynchronous solution. Observe that

$$\Pi'(w_0^*) = \frac{A}{-A + B} + C > -1 + C > -1, \tag{4.10}$$

where $A = (w_0^* - w^*)(\frac{\phi_S}{Ks_k})(2s_k)^{\phi_S/K} < 0$, $B = w_L'(s_k) > 0$, and $C = (w^* - w_0^*)(\frac{\phi_S}{\phi_A})(\frac{w_L'(s_k)}{w_L(s_k)})\frac{\partial s_k}{\partial w_0} > 0$. Given the equation (4.9), we can also rewrite (4.10) as

$$\Pi'(w_0^*) = \frac{A + D}{-A + B}$$

for A, B as above and $D = (2s_k)^{\phi_S/K}$. Thus, if (4.7) holds, then $\Pi'(w_0^*) < 1$, so the fixed point w_0^* is stable. This completes the proof of Proposition 1.

Remark 17. Equation (4.8) matches the geometry of the silent phase slow dynamics: when w_0 increases, the jump-up curve $w_L(s_{tot})$ is reached sooner, at a larger value of s_k. Thus geometrically, (4.8) encodes the competition between the fact that an increase in w_0 shortens τ_s, tending to diminish $\Pi(w_0)$, but also increases s_k, hence increasing the amount of time oscillator 2 spends in the active phase and tending to increase $\Pi(w_0)$.

Remark 18. In the limit of large K, condition (4.7) reduces to the inequality $1 < w_L'(s_k)$.

Remark 19. Given that $\Pi'(w_0^*) > -1$ from (4.10), we can refer to (4.8) to observe that $\Pi'(w_0^*) \in (-1, 0)$ if the simple condition $K s_k < \frac{w_L(s_k)\phi_A}{w_L'(s_k)}$ holds. This is of interest because it is analogous to the stability condition for Case II in [19]. If it holds for all s_k, then Π is monotone decreasing and has a unique fixed point, which is stable. Given that K is large, however, this condition may be difficult to satisfy.

Remark 20. We can obtain a different global stability condition by deriving a criterion for Π to be uniformly contracting on (w_{RK}, w^*). This entails finding a condition under which $|\Pi(w_0) - \Pi(w_0')| < |w_0 - w_0'|$ for any two initial conditions w_0, w_0' on $\{s_{tot} = 1/2\}$; see [1], [15]. This yields the more complicated condition that

$$|(w_L(s_k) - w^*)(s_k)^{\phi_S/K} - (w_L(s_k') - w^*)(s_k')^{\phi_S/K}| <$$

$$\left| (w_{RK} - w^*)(w_{RK})^{\phi_S/\phi_A} \left(\frac{(s_k)^{\phi_S/K}}{w_L(s_k)^{\phi_S/\phi_A}} - \frac{(s_k')^{\phi_S/K}}{w_L(s_k')^{\phi_S/\phi_A}} \right) \right|$$

for all $s_k, s_k' \in (0, 1/2)$.

Corollary 2. *The period $\mathcal{T}$ of an antisynchronous solution is*

$$\mathcal{T} = \ln \left[\left(\frac{1}{2s_k} \right)^{2/K} \left(\frac{w_L(s_k)}{w_{RK}} \right)^{2/\phi_A} \right]$$

$$= \ln \left[\left(\frac{w_L(s_k) - w^*}{w_0^* - w^*} \right)^{2/\phi_S} \left(\frac{w_L(s_k)}{w_{RK}} \right)^{2/\phi_A} \right]$$

$$= \ln \left[\left(\frac{w_{RK} - w^*}{w_0^* - w^*} \right)^{2/\phi_S} \right],$$

where $s_k = s_k(w_0^*)$

This follows from the definition of $\Pi(w_0)$, which implies that the period is given by $2(\tau_s + \tau_a)$, with the equalities coming from (4.3) and (4.5). It provides more explicit information about the influence of parameters on period than the expression given in Corollary 1 in Section 3.4. In Figure 12, we demonstrate this result by comparing the results of the first formula given for period $\mathcal{T}$ in Corollary 2 (solid line) with periods derived from numerical simulations (dashed line) of a mutually coupled network of the form (2.3) with direct inhibition (2.4). To employ the formula, we substituted the approximation

$$s_k(w_0) \approx 1/2 - \lambda(w_L(1/2) - w_0), \tag{4.11}$$

where λ denotes the slope of the approximately linear jump-up curve $w_L(s_{tot})$, into the fixed point equation (4.4) and solved numerically for w_0 as a function of K with ϕ_S, ϕ_A fixed. Then we used the resulting values $w_0(K)$ to solve for s_k from (4.11), which we plugged in to compute $\mathcal{T}$ as a function of K from the formula; we also set $w_L(s_k) = w_0$ in the formula. This latter substitution can be expected to hold for K large since w should not change much as inhibition decays. As it turns out, this substitution is quite accurate for more moderate K, since the increase in w
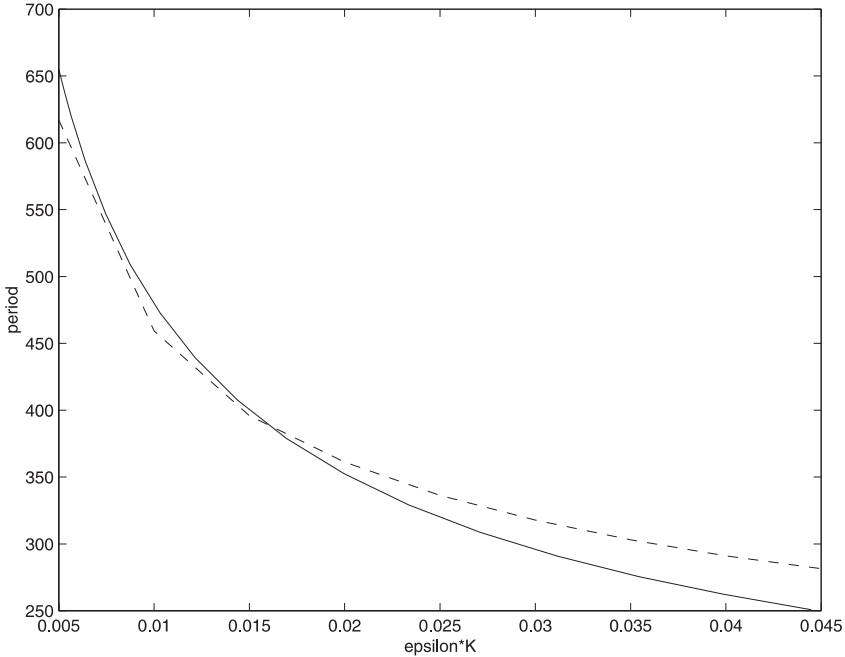
Fig. 12. Simulated (dashed) and approximate predicted (solid) period of antisynchronous oscillation, plotted versus decay rate of inhibition.

before $w_F(s_{tot})$ is crossed roughly cancels the decrease in w after the crossing. The error in the formula actually increases with K due to drift in w just before $w_L(s_{tot})$ is reached; this occurs because as s_k shrinks, so does $K s_k$, slowing the decay of inhibition relative to the rate of change of w.

   This analysis immediately generalizes to networks of arbitrary size: if there are N oscillators, then (4.7) gives a condition for stability between clusters for an anti-synchronous solution of 2 clusters of $N/2$ oscillators each. Conditions for stability within clusters for a larger network follow from the analysis of fully synchronized oscillators in [19] and in Appendix B of [13], taking into account that in a mutually coupled network, oscillators receive less inhibition in a clustered solution than in a synchronized one, since fewer oscillators fire in each oscillation.

4.2. Globally inhibitory networks and other extensions

The next issue to address is how the map Π changes relative to the above for a solution with antisynchronous E clusters, and a synchronized J population, in a globally inhibitory network. Under a few basic assumptions, we find that such a solution exists and is stable.

   We can arrange the dynamics of the J oscillators such that they fire and jump down following the firing and the falling down, respectively, of the active E cluster. The J then jump up to an excited level and jump down after the excitation has disappeared. Assume that both E clusters spend the same length of time, τ_a, in

the active phase after firing. If there are the same number of E oscillators in each cluster or the J dynamics in the active phase does not depend on the number of E oscillators exciting the J, then all J active phases will have a constant duration, as we assumed for much of Section 3. In this case, the total time from the activation of an E cluster to the moment when the resultant (indirect) inhibition felt by all of the E oscillators begins to diminish (via $\dot{s}_J = -Ks_J$) will be constant, call it τ_{act}.

Suppose that a solution consisting of two antisynchronous E clusters exists for large K and that one of the clusters, say E_1, jumps up to the active phase from the point $(w_L(s_k), s_k)$. The time τ_a that E_1 subsequently spends in the active phase may be computed from the evolution of $\dot{w} = -\phi_A w$ with the boundary values $w(0) = w_L(s_k)$ and $w(\tau_a) = w_{RK}$, which yields

$$\tau_a = \frac{1}{\phi_A} \ln(\frac{w_L(s_k)}{w_{RK}}).$$

The additional time until $\dot{s}_J = -Ks_J$ kicks in is then $\tau_{inh} = \tau_{act} - \tau_a$. With the same definitions as earlier (but $w^* = w_F(1)$), $\Pi(w_0)$ is given by the evolution of $\dot{w} = \phi_S(w^* - w)$, with $w(0) = w_{RK}$, for time $\tau_{inh} + \tau_s + \tau_a = \tau_{act} + \tau_s$. This yields

$$\Pi(w_0) = w^* + (w_{RK} - w^*)e^{-\phi_S \tau_{act}}(2s_k)^{\phi_S/K}.$$

Here, s_k is defined by

$$w_L(s_k) = w^* + (w_0 - w^*)e^{-\phi_S \tau_{inh}}(2s_k)^{\phi_S/K}. \tag{4.12}$$

This gives a fixed point equation which can be written as

$$(w_0 - w^*)^2 = (w_{RK} - w^*)(w_L(s_k) - w^*)\left(\frac{w_{RK}}{w_L(s_k)}\right)^{\phi_S/\phi_A}. \tag{4.12}$$

As in the previous subsection, we can see that this has a solution by observing that at $w_0 = w^*$, the left hand side of (4.12) is less than the right hand side, while at $w_0 = w_{RK}$ (or $w_0 = w_{esc}$ as in Remark 15) the opposite holds. This last fact follows since

$$\frac{w_{RK} - w^*}{w_L(s_k) - w*} > 1 > \left(\frac{w_{RK}}{w_L(s_k)}\right)^{\phi_S/\phi_A}.$$

Likewise,

$$\Pi'(w_0) = (w_{RK} - w^*)e^{-\phi_S \tau_{act}}(2s_k)^{\phi_S/K}\left(\frac{\phi_S}{Ks_k}\right)\frac{\partial s_k}{\partial w_0}$$

where $\frac{\partial s_k}{\partial w_0}$ depends on w_0 and can be obtained from (4.12). In fact, using the notation in (4.10), $\Pi'(w_0^*) = A/(-A + B)$ at an arbitrary fixed point w_0^*, so all fixed points are stable.

Remark 21. Above, we have assumed a constant length of active phase for each firing E cluster and a corresponding fixed length of active phase for the J population. The analysis becomes more complicated if we allow the duration of the E and J active phases to depend on s_k, w_0, and the number of E oscillators per cluster.

Remark 22. We have also extended the computation of the map $\Pi(w_0)$ and its derivative to a mutually coupled network with *indirect* coupling and to networks having an additional variable that evolves on the slow time scale in the silent phase (and on the fast time scale in the silent phase). Although these changes require additional notation and calculations, there is no technical obstacle to these or similar extensions. We leave the details to the interested reader.

5. Discussion

In this paper, we prove that certain conditions imply the existence and stability of clustered solutions for mutually coupled and globally inhibitory networks of oscillators with synaptic coupling. The models that we analyze and the assumptions that we make about them are motivated by biological experiments on certain synaptically coupled neuronal networks, exemplified by those involved in thalamic sleep rhythms. In the context of sleep rhythms, clustered solutions correspond to what are known as spindling states, in which clusters of excitatory thalamocortical relay cells take turns firing along with a population of inhibitory thalamic reticular cells [6], [16], [17]. Since thalamic reticular cells are known to have longer active states than relay cells [4], we assume that the J oscillators in our globally inhibitory networks are active longer than the E. There are also many examples of mutual inhibitory connections in the nervous system; in fact, since thalamic reticular cells inhibit each other, our mutually inhibitory network can be taken as a reduced model for reticular interactions during periods of quiescence of relay cells [5].

The results given in Section 3 provide existence and stability conditions that are stated in terms of a balance of time lengths. These times are associated with intrinsic properties of the oscillators and their coupling and arise naturally in our geometric analysis. Many model parameters have clear relations to the time lengths of interest. For example, changes in the inhibitory decay rate directly effect changes in the decay time τ_S, while parameters that alter the speed with which oscillators evolve in the active phase directly influence the active phase durations τ_E and τ_J. Many of the results that we present were based on simplifying assumptions made for ease of notation and clarity. There is no technical obstacle to removing these as desired, as demonstrated in Section 3.6.

In Section 4, we derive a map with a fixed point that is an antisynchronous solution, state a stability condition for any such solution, and provide a formula for the period of antisynchronous oscillations. This requires additional assumptions on the models, but in return we obtain results given directly in terms of model parameters and phase space structures that are directly linked to model parameters. The results in both sections can be used to generate clustered states numerically, to compute information about these states, or to predict how changes in parameters will affect the stable states of a system. The explicit results in Section 4 may be especially useful in that they offer insight into the effects of relatively subtle changes in parameters, such as changes in parameters in $f(v, w)$ that affect the position or shape of the cubic v-nullclines.

Our results show that the combination of a short J active phase (relative to that needed for a stable synchronous solution) and a relatively fast decay of inhibition

promotes stable clustered solutions in globally inhibitory networks. To sustain any oscillation involving a synchronized J population in such networks, it is necessary to have a sufficiently fast J recovery so that the J are ready to fire in response to the excitation they receive from E firing; this is especially true when the decay of inhibition that releases the E is fast. While the rate of evolution of the E in the silent phase also affects the number of clusters that can coexist, this rate does not affect the period of a clustered solution of a fixed type; a period consists entirely of alternating J active phases and phases of decay of inhibition.

In some sleep states, it may be that a slowly decaying form of inhibition is the dominant form of coupling to the relevant E population (the relay cells) [17], [18]. If we gradually decrease the size of K_J to model this slower decay, then the E oscillators can experience larger and larger changes in their w-values as inhibition decays. Such effects may result in suppression of particular clusters or other more exotic solutions. Alternately, a global synchronization mechanism may arise
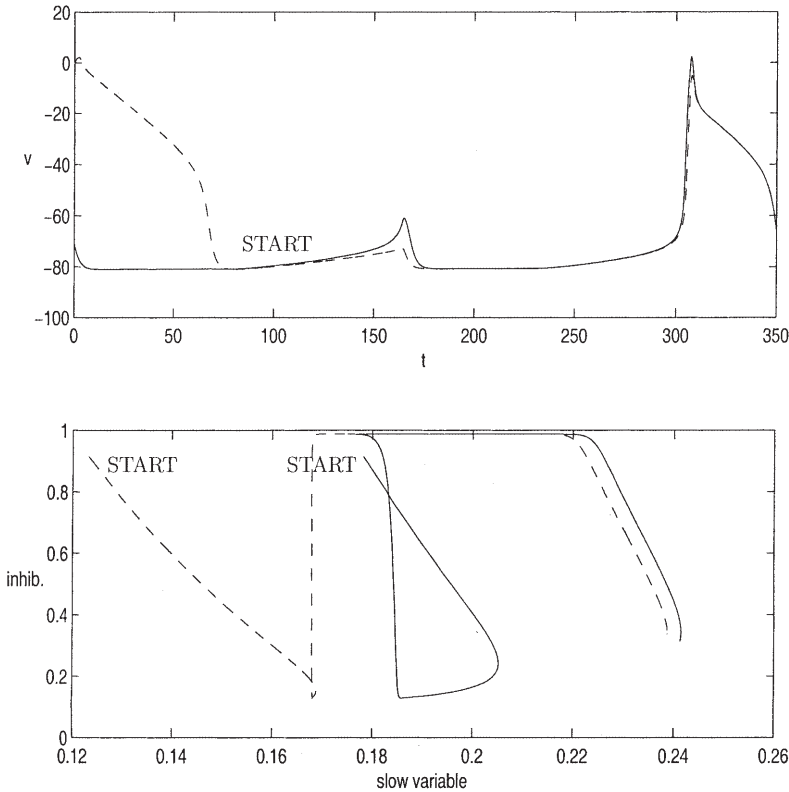
Fig. 13. A global synchronization mechanism. Top: voltage versus time for two different E clusters in a network that begins in the 3-cluster state. The label START marks the start of the time interval on which the curves in the bottom figure are defined. Bottom: projection of the trajectories of these clusters to (w, s_J) space. After the dashed cluster fires (not shown), it catches up to the solid cluster.

in which non-firing oscillators experience great declines in w as inhibition decays, such that their w values are still near w_{RK} when a firing group jumps down.

Figure 13 displays a related phenomenon, in which a non-firing cluster (solid line) experiences a sizeable decrease in w during a period of inhibitory decay, such that another cluster (dashed line) catches up to it; this was generated with the same equations and parameters as Figures 6 and 8-10 but with smaller K_J. In the context of the n-cluster solutions considered in this paper, a comparison of the flow of (3.1) to that of (3.2) proves that slow decay of inhibition enhances compression *within* clusters in the silent phase. At the same time, slow decay of inhibition may pull separate clusters closer together, as in Figure 13, having an overall effect of destabilizing a clustered state in favor of a synchronous state or a state with fewer clusters. The full treatment of these effects would require combining the analysis in this paper with that in [13] and [19].

References

1. Bose, A., Booth, V., Recce, M.: A temporal mechanism for generating the phase precession of hippocampal place cells. J. Comput. Neurosci., **9**, 5–30 (2000)
2. Destexhe, A., Mainen, Z.F., Sejnowski, T.J.: Kinetic models of synaptic transmission. In C.Koch and I. Segev, editors, Methods in Neuronal Modeling: From Ions to Networks, pages 1–25. The MIT Press, Cambridge, MA, second edition (1998)
3. Destexhe, A., McCormick, D.A., Sejnowksi, T.J.: A model for 8-10 Hz spindling in interconnected thalamic relay and reticularis neurons. Biophys. J., **65**, 2474–2478 (1993)
4. Destexhe, A., Sejnowski, T.: Synchronized oscillations in thalamic networks: insights from modeling studies. In M. Steriade, E. Jones, and D. McCormick, editors, Thalamus, Volume II, pages 331–372. Elsevier, Amsterdam (1997)
5. Golomb, D., Wang, X.-J., Rinzel, J.: Synchronization properties of spindle oscillations in a thalamic reticular nucleus model. J. Neurophysiol., **72**, 1109–1126 (1994)
6. Huguenard, J.: Anatomical and physiological considerations in thalamic rhythm generation. J. Sleep Res., **7**, Supplement **1**, 24–29 (1998)
7. Kandel, E.R., Schwartz, J.H., Jessell, T.M.: Principles of Neural Science. Appleton & Lange, Norwalk, Conn. (1991)
8. LoFaro, T., Kopell, N.: Timing regulation in a network reduced from voltage-gated equations to a one-dimensional map. J. Math. Biol., **38**, 479–533 (1999)
9. Mischenko, E.F., Rozov, N.Kh.: Differential Equations with Small Parameters and Relaxation Oscillations. Plenum Press, New York and London (1975)
10. Rinzel, J., Ermentrout, G.B.: Analysis of neural excitability and oscillations. In C. Koch and I. Segev, editors, Methods in Neuronal Modeling: From Ions to Networks, pages 251–291. The MIT Press, Cambridge, MA, second edition (1998)
11. Rubin, J., Terman, D.: Geometric singular perturbation analysis of neuronal dynamics. In B. Fiedler, G. Iooss, and N. Kopell, editors, Handbook of Dynamical Systems, vol. 3: Towards Applications. Elsevier. To appear.
12. Rubin, J., Terman, D.: Geometric analysis of population rhythms in synaptically coupled neuronal networks. IMA Preprint Series # 1586 (1998)
13. Rubin, J., Terman, D.: Geometric analysis of population rhythms in synaptically coupled neuronal networks. Neural Comput., **12**, 597–645 (2000)

14. Skinner, F., Kopell, N., Marder, E.: Mechanisms for oscillation and frequency control in networks of mutually inhibitory relaxation oscillators. J. Comput. Neurosci., **1**, 69–87 (1994)
15. Somers, D., Kopell, N.: Rapid synchronization through fast threshold modulation. Biol. Cybern., **68**, 393–407 (1993)
16. Steriade, M., Jones, E., McCormick, D.: editors. Thalamus, Volume II. Elsevier, Amsterdam (1997)
17. Steriade, M., McCormick, D.A., Sejnowski, T.J.: Thalamocortical oscillations in the sleep and aroused brain. Science, **262**, 679–685 (1993)
18. Terman, D., Bose, A., Kopell, N.: Functional reorganization in thalamocortical networks: Transition between spindling and delta sleep rhythms. Proc. Natl. Acad. Sci. USA, **93**, 15417–15422 (1996)
19. Terman, D., Kopell, N., Bose, A: Dynamics of two mutually coupled inhibitory neurons. Physica D, **117**, 241–275 (1998)
20. Terman, D., Lee, E.: Partial synchronization in a network of neural oscillators. SIAM J. Appl. Math., **57**, 252–293 (1997)
21. Terman, D., Wang, D.L.: Global competition and local cooperation in a network of neural oscillators. Physica D, **81**, 148–176 (1995)
22. Wang, X.-J., Rinzel, J.: Alternating and synchronous rhythms in reciprocally inhibitory model neurons. Neural Comput., **4**, 84–97 (1992)